Calcite precipitation from aqueous solutions with different calcium and hydrogen carbonate concentrations

Kai Zeppenfeld

ABSTRACT

This paper describes the influence of different Ca^{2+} and HCO_3^- concentrations on the precipitation of calcite in aqueous solutions. Mixtures of $CaCl_2$ and $NaHCO_3$ solutions with different concentrations were stirred, covering a wide range of supersaturation and precipitation of calcite. The resulting reduction of the Ca^{2+} concentration was recorded as a function of time by measuring the electric conductivity and the pH value. The nucleation rate increased with increasing supersaturation and can be described with the classical theory of nucleation. For different solutions with similar values of supersaturation, the hydrogen carbonate/calcium ratio had no significant influence on the rate of nucleation. At a given calcium concentration the precipitation rate increased with increasing supersaturation. This effect was more pronounced at higher supersaturations. Measurements at similar values of supersaturation showed that the calcite precipitation rate increased with increasing hydrogen carbonate/calcium ratio. These results can be explained by applying a surface complexation model. The crystal surface concentrations of the two species $>CaCO_3^-$ and $>CO_3^-$ and the adsorption of $CaCO_3^0$ ion pairs are responsible for catalysing calcite precipitation.

Key words | calcite precipitation, crystal growth, hydrogen carbonate/calcium ratio, nucleation, supersaturation, surface complexation

Kai Zeppenfeld
Scientific Consultant
Schottlandstr. 4a,
D-59368 Werne,
Germany
Tel.: +49 2389 927458
Fax: +49 2389 533662
E-mail: *drkaizepp@t-online.de*

INTRODUCTION

The precipitation of calcite ($CaCO_3$) is of great importance in natural environments, regulating the carbon composition of rivers, lakes and oceans (Stumm & Morgan 1996). Moreover $CaCO_3$ scaling is often a major problem in natural water supply of industrial plants and various chemical engineering processes. The precipitation and crystallization of calcite as an insulating layer causes a decrease in the flow rate in pipes and reduced heat transfer in heat exchangers (Drew Ameroid 1997). Several publications report on the crystallization of $CaCO_3$ in aqueous solutions. Apart from the temperature (Kabasaci *et al.* 1996; Johannsen *et al.* 1997), the pH value (Brown *et al.* 1993; Gomez-Morales *et al.* 1996) and the number of inoculating seed crystals (Reddy & Gaillard 1981; Takasaki *et al.* 1994) the crystal growth rate is strongly dependent on supersaturation with respect to calcite. With increasing supersaturation S the growth rate r follows an expression of the form $r \sim (S-1)^x$. Therefore r corresponds to a linear ($x = 1$) (Reddy & Nancollas 1971; Meyer 1979; Gutjahr *et al.* 1996) or parabolic ($x = 2$) dependence (Kazmierczak *et al.* 1982; Nielsen & Toft 1984; Lioliou *et al.* 2007) on the degree of supersaturation.

In addition, the kinetics of calcite precipitation is widely explained by surface reaction-controlled mechanisms. The surface reaction-controlled mechanisms consist of adsorption, dehydration and surface diffusion of lattice ions, spiral growth at screw dislocations, or two-dimensional nucleation on the mineral surface. The precipitation of calcite can also be diffusion controlled, depending on the degree of supersaturation and hydrodynamic conditions at which

doi: 10.2166/aqua.2010.076

the precipitation is initiated (Shiraki & Brantley 1995; Zeppenfeld 2005).

Apart from supersaturation, the growth rate of calcite may also be affected by the aqueous composition through the carbonate anion to calcium cation concentration ratio of the solution (van der Weijden *et al.* 1997; Lin & Singer 2005). These studies demonstrated that for different solution compositions with the same degree of supersaturation, the calcite precipitation rate increased with increasing carbonate/calcium ratio. This finding contradicts the generally accepted assumption that the degree of supersaturation is the sole factor for controlling precipitation kinetics. The precipitation experiments were initiated by adding calcite seed crystals to the solutions in a constant pH range from 7.2 to 9.0. Furthermore it could be demonstrated (Nehrke *et al.* 2007) that under a high and fixed pH (10.2) and at a constant degree of supersaturation, the growth rate of a single crystal was highest when the concentration ratio CO_3^{2-}/Ca^{2+} of the solution equalled one. The growth rate decreased proportionally with positive or negative deviation of the CO_3^{2-}/Ca^{2+} ratio from one.

In the current study the precipitation rates of calcite were measured as a function of supersaturation at different concentrations of hydrogen carbonate and calcium ions in non-seeded and homogeneous solutions. The unexpected results may explain the deposition of calcite in natural water systems and in natural water supply under conditions where Ca^{2+} and HCO_3^- are present as major components.

MATERIALS AND METHODS

All experiments were carried out in a 500 cm^3 glass vessel thermostatized at a constant room temperature of 25 ± 0.5°C. $NaHCO_3$ and $CaCl_2$ solutions were prepared from corresponding reagent grade crystalline solids (Merck) using deionised water (0.06 $\mu S\,cm^{-1}$). The concentration of the $CaCl_2$ and $NaHCO_3$ solutions were 5.0 to 9.0 $mmol\,l^{-1}$ and 6.0 to 20.0 $mmol\,l^{-1}$, respectively. Equal volumes (200 ml) of the calcium chloride and hydrogen carbonate solutions were rapidly mixed by injecting them at the same time under stirring (600 rpm) using a magnetic stirrer to achieve a critical supersaturation with respect to $CaCO_3$. The magnetic stirrer has no noticeable influence on $CaCO_3$ precipitation, as substantially higher intensities of a magnetic field (> 0.2 tesla) are needed for a noticeable effect (Tai *et al.* 2008). All systems were operated open, which included the exchange of CO_2 with the atmosphere. The initial pH value of all mixed solutions ranged from 8.22 to 8.38, measured by a WTW 320 pH meter (Merck Labor und Chemie Vertrieb West GmbH, Bochum, Germany). The electric conductivity was measured using a WTW 318 instrument (Merck Labor und Chemie Vertrieb West GmbH, Bochum, Germany). The conductivities of all prepared solutions ranged from 875 to 1,810 $\mu S\,cm$. Before each new experiment the glass vessel was washed with hydrochloric acid and dried thoroughly.

κ_{25} alterations in the Ca^{2+} concentration $\Delta[Ca^{2+}]$ in the solution were followed according to Equation (1) based on electric conductivity measurements.

$$\Delta[Ca^{2+}] = (\kappa_{25}^0 - \kappa_{25})/\Lambda_{molar} \quad (1)$$

κ_{25}^0 is the electric conductivity of the solutions immediately after mixing and Λ_{molar} denotes the average molar equivalent conductivity. A value of 180 ± 3 $S\,cm^2\,mol^{-1}$ was calculated for $Ca(HCO_3)_2$ solutions in the described concentrations range (Landolt & Börnstein 1960; Zeppenfeld 2001). The low concentrations dependency of Λ_{molar} (Onsager & Fuoss 1932), causing an error of ±3 $S\,cm^2\,mol^{-1}$ was neglected. In addition, an additional low dependency on dissolved CO_2 (House 1981) and NaCl causing a maximal error of 2%, was also neglected.

The conditions of the supersaturated solutions were selected so that the formation of calcium carbonate was initiated after an induction time. The onset of precipitation was accompanied by a reduction in the Ca^{2+} concentration, which was determined by measuring the electric conductivity κ_{25} as a function of time. The crystalline precipitation products were dried at room temperature and examined by X-ray powder diffractometry. The precipitate consisted only of calcite; the aragonite and the vaterite modifications were not observed.

RESULTS AND DISCUSSION

Kinetics of calcite precipitation

The calcite precipitation described above is considered to result from the following reactions:

$$CaCO_3(s) \leftrightarrow Ca^{2+} + CO_3^{2-} \quad K_{so} \tag{2}$$

$$CaCO_3(s) + H^+ \leftrightarrow Ca^{2+} + HCO_3^- \quad K_{so} K_2^{-1} \tag{3}$$

$$CaCO_3(s) + H_2CO_3 \leftrightarrow Ca^{2+} + 2HCO_3^- \quad K_{so} K_1 K_2^{-1} \tag{4}$$

The supersaturation S with respect to calcite is defined as:

$$S = \frac{a(Ca^{2+})_t \, a(CO_3^{2-})_t}{K_{so}} = \frac{a(Ca^{2+})_t \, a(HCO_3^-)_t}{a(H^+)_t \, K_{so} \, K_2^{-1}}$$

$$= \frac{a(Ca^{2+})_t \, a^2(HCO_3^-)_t}{a(H_2CO_3)_t \, K_{so} \, K_1 \, K_2^{-1}} \tag{5}$$

where K_{so} is the thermodynamic solubility product of calcite ($pK_{so} = 8.42$ (Stumm & Morgan 1996)), K_1 the first acidity constant of H_2CO_3 ($pK_1 = 6.35$), K_2 the second acidity constant of H_2CO_3 ($pK_2 = 10.30$), $a(\,)_t$ the activities of the ions in the solution at time t, with the activity coefficients γ_z determined by the Davies Equation (Stumm & Morgan 1996):

$$-\log \gamma_z = 0.51 z^2 [I^{0.5}/(1 + I^{0.5}) - 0.3I] \tag{6}$$

in which I is the ionic strength and z the charge of the corresponding ion.

The resulting Ca^{2+} and HCO_3^- concentrations of all mixed solutions and the values of the supersaturation S calculated for an average initial pH of 8.30 (Equation (5)) are summarized in Table 1. Five calcium concentrations between 2.5 and 4.5 mmol l^{-1} were combined with hydrogen carbonate concentrations between 3.0 and 10.0 mmol l^{-1}. The supersaturation increased with increasing calcium and increasing hydrogen carbonate concentration, whereby similar values of S can result from quite different hydrogen carbonate/calcium concentration ratios.

Figure 1 shows the time-related alteration in the Ca^{2+} concentration for a solution with 4.0 mmol l^{-1} Ca^{2+} and 5.0 mmol l^{-1} HCO_3^- and a supersaturation of 27.9. The alteration of the pH value with time is also shown. Because a certain supersaturation was achieved, the first stable nuclei were formed. These were growing to a detectable size while the formation of new nuclei was going on (Söhnel & Mullin 1988) and the Ca^{2+} concentration and the pH value were decreasing slowly, resulting in a slightly turbid solution. After the formation of a sufficient area of nuclei, the crystal growth was the dominant process (Mullin 2001) and mass precipitation of calcite started, followed by a rapid decrease in the Ca^{2+} concentration. A drop in the pH value indicated the beginning of precipitation according to Equations (3) and (4), whereby the dissolved CO_2 was stripped partially by stirring and therefore a final pH value of 7.43 was attained at 160 min. The supersaturation decreased according to Equation (5) and a final value of $S = 1.3$ could be calculated. Therefore the solution was still supersaturated and the dissolution reaction of $CaCO_3$ could be neglected. This was valid for all experimental runs.

The required time for the initiation of calcite mass precipitation, in particular the turning point in the Ca^{2+} concentration versus time function, which was determined by a geometric method, is referred to as the induction period, t_{Ind} (60 min). Table 1 shows the induction period at various values of supersaturation S and the hydrogen carbonate/calcium ratio. With increasing supersaturation the induction period decreased because higher supersaturation promotes the formation of nuclei (Mullin 2001). At a similar degree of supersaturation e.g. $S \cong 22$ or $S \cong 33$ the hydrogen carbonate/calcium ratio had no significant influence on the nucleation, as the values of the induction period were comparable.

The precipitation of calcite (Figure 1) follows a rate expression of the form

$$-\frac{d[Ca^{2+}]}{dt} = k([Ca^{2+}] - [Ca^{2+}]_0)^2 \tag{7}$$

where k (l/mmol min) is the rate constant of precipitation, $[Ca^{2+}]_0$ is the concentration of calcium ions before precipitation is started and $[Ca^{2+}]$ is the Ca^{2+} concentration measured at time t.

Analysis of calcite crystal growth data is facilitated by the integrated form of Equation (7):

$$\frac{1}{[Ca^{2+}]} - \frac{1}{[Ca^{2+}]_0} = kt \tag{8}$$

The linear plot of $1/[Ca^{2+}] - 1/[Ca^{2+}]_0$ versus time presented in Figure 1 confirms that Equation (8) is valid to interpret the experimental results. The rate constants

Table 1 | Calculated values of the rate constant k and the induction period t_{Ind} versus the different Ca^{2+} and HCO_3^- concentrations, the resulting supersaturations S (pH = 8.30) and the hydrogen carbonate/calcium concentration ratio $[HCO_3^-]/[Ca^{2+}]$. The errors in the value of the figures in the right-hand column are shown in parentheses

$[Ca^{2+}]$ (mmol l^{-1})	$[HCO_3^-]$ (mmol l^{-1})	$[HCO_3^-]/[Ca^{2+}]$	S	t_{Ind} (min)	k 10^{-4} (l/mmol min)
2.5	4.0	1.600	15.4	270	4.2 (0)
2.5	4.5	1.800	17.1	205	6.5 (0)
2.5	5.0	2.000	18.8	170	9.2 (1)
2.5	5.5	2.200	20.6	140	11.4 (1)
2.5	6.0	2.400	22.3	120	13.7 (1)
2.5	6.5	2.600	23.9	110	15.3 (1)
2.5	7.0	2.800	25.5	95	17.3 (2)
2.5	7.5	3.000	27.0	70	21.3 (3)
2.5	8.0	3.200	28.5	55	26.1 (2)
2.5	8.5	3.400	30.1	43	31.5 (3)
2.5	9.0	3.600	31.6	34	36.0 (3)
2.5	9.5	3.800	33.0	27	39.7 (4)
2.5	10.0	4.000	34.5	22	44.8 (5)
3.0	4.0	1.333	18.0	205	4.7 (1)
3.0	4.5	1.500	20.0	165	6.3 (1)
3.0	5.0	1.667	22.0	140	8.3 (0)
3.0	5.5	1.833	24.0	120	10.2 (1)
3.0	6.0	2.000	25.9	95	14.1 (1)
3.0	6.5	2.167	27.9	65	17.4 (2)
3.0	7.0	2.333	29.8	50	21.6 (2)
3.0	7.5	2.500	31.7	35	25.1 (2)
3.0	8.0	2.667	33.6	28	27.5 (2)
3.0	8.5	2.833	35.5	21	31.2 (3)
3.0	9.0	3.000	37.0	17	33.4 (4)
3.0	9.5	3.167	38.8	14	37.0 (3)
3.0	10.0	3.333	40.6	12	39.6 (3)
3.5	3.5	1.000	17.9	210	2.3 (0)
3.5	4.0	1.143	20.4	150	4.1 (0)
3.5	4.5	1.286	22.7	120	5.5 (0)
3.5	5.0	1.429	25.1	100	7.1 (1)
3.5	5.5	1.571	27.3	80	10.0 (1)
3.5	6.0	1.714	29.5	60	12.3 (1)
3.5	6.5	1.857	31.8	40	14.8 (1)
3.5	7.0	2.000	33.9	30	16.9 (1)
3.5	7.5	2.143	36.1	25	19.7 (2)
3.5	8.0	2.286	38.3	20	21.8 (3)
3.5	8.5	2.429	40.4	16	24.3 (2)
3.5	9.0	2.571	42.5	13	26.9 (3)
3.5	9.5	2.714	44.3	11	29.1 (3)
3.5	10.0	2.857	46.4	10	31.2 (4)
4.0	3.0	0.750	17.3	280	0.8 (1)
4.0	3.5	0.875	20.0	170	2.1 (0)
4.0	4.0	1.000	22.7	115	3.5 (0)
4.0	4.5	1.125	25.3	85	4.6 (1)
4.0	5.0	1.250	27.9	60	7.0 (1)
4.0	5.5	1.375	30.5	42	9.6 (1)
4.0	6.0	1.500	33.0	32	11.5 (1)
4.0	6.5	1.625	35.4	26	13.3 (2)
4.0	7.0	1.750	37.9	21	15.1 (2)
4.0	7.5	1.875	40.4	17	16.9 (2)
4.0	8.0	2.000	42.7	15	18.4 (2)
4.0	9.0	2.250	47.5	11	23.1 (3)
4.0	10.0	2.500	52.1	9	27.0 (3)
4.5	3.0	0.667	19.1	220	0.5 (0)
4.5	3.5	0.778	22.0	150	1.5 (0)
4.5	4.0	0.889	24.9	120	2.3 (1)
4.5	4.5	1.000	27.9	100	3.2 (0)
4.5	5.0	1.111	30.7	65	4.7 (0)
4.5	5.5	1.222	33.5	45	6.4 (1)
4.5	6.0	1.333	36.4	32	8.3 (1)
4.5	6.5	1.444	39.0	25	10.1 (1)
4.5	7.0	1.556	41.8	21	11.5 (1)
4.5	7.5	1.667	44.5	17	13.3 (1)
4.5	8.0	1.778	47.1	14	15.2 (1)
4.5	9.0	2.000	52.4	10	18.9 (2)
4.5	10.0	2.222	57.4	8	21.7 (3)

k calculated via Equation (8) as a function of supersaturation S and different hydrogen carbonate/calcium ratios are listed in Table 1. With increasing supersaturation the rate constant increased, whereby at similar values of supersaturation e.g. $S \cong 22$ or $S \cong 33$ the rate constant increased with increasing hydrogen carbonate/calcium ratio.

Nucleation

The formation of nuclei is the first step to produce a crystalline product. Nucleation mechanisms are considered to be either homogeneous, where collisions on the

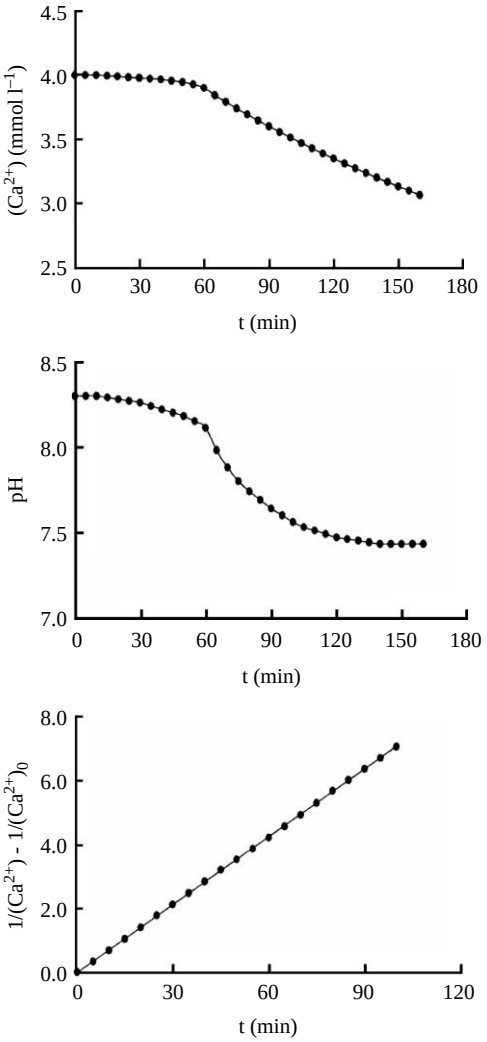

Figure 1 | Time versus Ca^{2+} concentration (top), the time-related alteration in the pH value (middle) and the parameter $1/[Ca^{2+}] - 1/[Ca^{2+}]_0$ versus time (bottom) for a prepared solution with 4.0 mmol l^{-1} Ca^{2+} and 5.0 mmol l^{-1} HCO_3^-.

molecular scale lead to the generation of nuclei, or heterogeneous, where surfaces of foreign solids catalyse the generation of nuclei. The rate of nucleation, J_s, in particular the number of nuclei per unit time per unit volume can be expressed as follows (Mersmann *et al.* 2000; Mullin 2001):

$$J_s = \Omega \exp\left[-\frac{16\pi V_m^2 \gamma^3 f(\Theta)}{3(K_B T)^3 \ln^2 S}\right] \tag{9}$$

in which V_m is the molar volume of calcite, γ the interfacial tension or surface energy of the solid in contact with the solution, K_B the Boltzmann constant, T the temperature, S the supersaturation and Ω the pre-exponential factor. For heterogeneous nucleation the surface energy is corrected by the factor $f(\Theta)$ which is related to the hypothetical contact angle of a solute nucleus spreading on the surface of a foreign particle. The contact angle is a function of the affinity between a cluster of the condensed solute and the uppermost layer of molecules of foreign particles, e.g. dust particles. For $f(\Theta) = 1$, the nucleation is homogeneous and for $f(\Theta) < 1$, the nucleation is heterogeneous.

If nucleation is followed by diffusional growth, the rate of nucleation J_s is reversely proportional to the induction period t_{Ind} (Söhnel & Mullin 1988):

$$t_{\mathrm{Ind}} = J_s^{-1} \tag{10}$$

Substituting Equation (10) into Equation (11) and rearranging results produces

$$\log t_{\mathrm{Ind}} = B(\log S)^{-2} - \log\Omega \tag{11}$$

with

$$B = \frac{16\pi V_m^2 \gamma^3 f(\Theta)}{3(K_B T)^3 \ln^2 10} \tag{12}$$

The plot of the dependence of the measured induction times (Table 1) as a function of supersaturation for the five different Ca^{2+} concentrations of the solutions is shown in Figure 2. The experimental data demonstrate that the log t_{Ind} versus $(\log S)^{-2}$ function is linear, whereby the dependence can be separated into two linear parts with different slopes. This observed dependence results from the fact that at low values of supersaturation ($S < 25$) the nucleation is predominantly heterogeneous ($f(\Theta) < 1$), whereas at high values of supersaturation ($S > 25$) homogeneous nucleation prevails ($f(\Theta) = 1$). The two linear parts, corresponding to the different nucleation mechanisms, are expected to have different slopes ($B_{\mathrm{hom}} > B_{\mathrm{het}}$) as can be determined from Equation (12) and as found experimentally (Figure 2). These results are in good agreement with earlier published investigations by Söhnel & Mullin (1978), who determined induction periods of $CaCO_3$ precipitation as a function of supersaturation.

Furthermore, it could be demonstrated that different Ca^{2+} concentrations and the resulting hydrogen carbonate/calcium ratio have no significant effect on heterogeneous

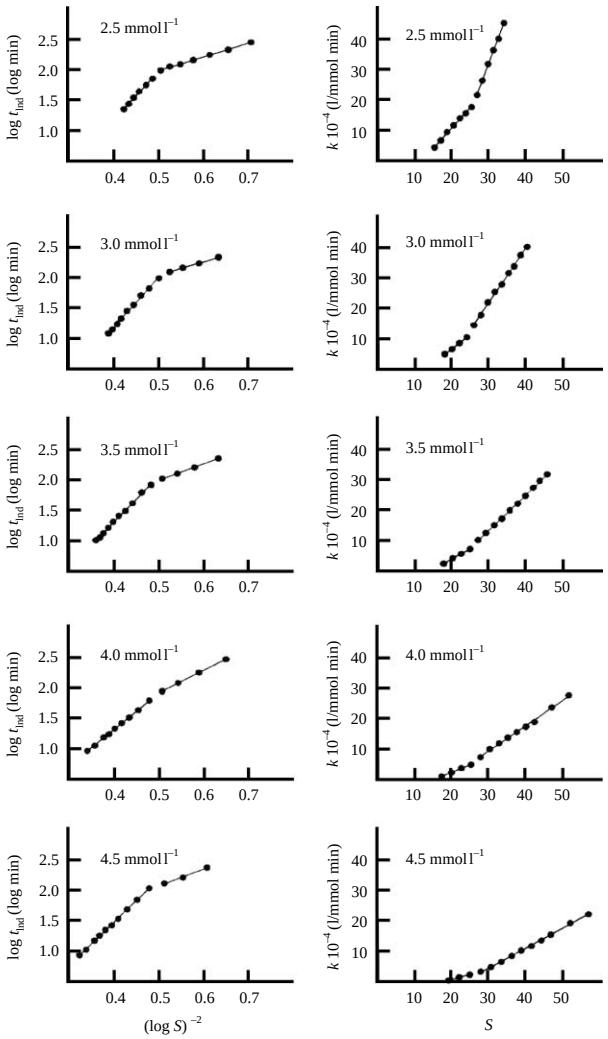

Figure 2 | Induction period t_{ind} (left column) and the calculated rate constant k (right column) as a function of supersaturation S for the five different Ca^{2+} concentrations of the solutions.

or homogeneous nucleation, because the slopes of the linear parts (B_{hom} and B_{het}) are similar (Figure 2). Thus the rate of nucleation or the induction period is only dependent on supersaturation, expressed by Equation (9).

Crystal growth

As soon as enough stable nuclei have formed they begin to grow into calcite crystals of visible size. There are two steps in mass deposition: first a transport process, whereby solute ionic species are transported from the bulk of the fluid phase to the surface of solids (nuclei and growing crystals). This is followed by an integration reaction with solute species arranging themselves into the crystal lattice (Mersmann *et al.* 2000; Mullin 2001). The transport process determines the number of contacts resulting in crystal growth. If the stirrer speed is sufficiently high, the crystal growth is primarily determined by the integration of the solute species into the crystal lattice. At slower stirrer speeds the rate controlling mechanism change continuously from surface reaction control to primarily transport control (Zeppenfeld 2005). Because of the constant kind of stirring (600 rpm in all experiments) and the resulting constant transport process, the change of the crystal growth rate is only controlled by processes on the crystal surface and increases with increasing supersaturation.

For small supersaturation ($S \geq 1$) the system may be contained near the thermodynamic equilibrium. Based on the minimum of free energy, the crystal surfaces are very smooth. If a single ion is added to this surface, it can form a bond with only its nearest neighbour, resulting in a very low binding energy, which is a major barrier for crystal growth. With increasing supersaturation the roughness of the crystal surfaces increases on the basis of a development of screw dislocations (Dove & Hochella 1993) and finally of two-dimensional and polynuclear growth (Shiraki & Brantley 1995). Any molecule incident on a rough crystal surface has a greater probability of ending up with a higher binding energy than a crystal with a smooth surface. The rough surfaces tend to maintain their roughness during growth and molecules attach themselves at sites, creating new corners which are preferred sites for subsequent additions (Nielsen 1984). With increasing degree of supersaturation the growth rate increases with different exponents, respectively. A parabolic dependence appears only at small supersaturation ($S \leq 1.5$). With increasing supersaturation ($S \geq 2.2$) the dependence becomes linear, whereby the crystal growth is strongly dependent on the roughness of the crystal surfaces (Mersmann *et al.* 2000; Teng *et al.* 2000).

Figure 2 shows the experimental rate constant k, or the precipitation rate as a function of supersaturation S, for the solutions with the five different Ca^{2+} concentrations listed in Table 1. With increasing hydrogen carbonate concentration and thereby increasing supersaturation the rate constant increased linearly. Therefore, it can be concluded that the growth rate increases with increasing roughness

of the surfaces and the crystal growth is mostly determined by two-dimensional and polynuclear growth. This experimental correlation can be separated into two linear parts with different slopes. At low supersaturation ($S < 25$) the slopes are substantially smaller than at higher supersaturation ($S > 25$). This dependence results from the fact that at low supersaturation the nucleation mechanism is heterogeneous whereas at higher supersaturation homogeneous nucleation prevails. The homogeneous nucleation results in an increasing formation of nuclei (Equation (9)), whereby the enhanced solid surfaces of nuclei promote the two-dimensional and polynuclear crystal growth.

Figure 2 shows that the slopes for both separated linear parts of the function $k(S)$ decrease with increasing Ca^{2+} concentration. The slope $m = dk/dS_{[Ca^{2+}]}$ characterizes how the rate constant increases, i.e. how much for a given Ca^{2+} concentration the precipitation is accelerated with supersaturation increase, which (owing to the experimental set up) corresponds to an increasing hydrogen carbonate/calcium ratio. A plot of m, calculated by linear regression, at the five different Ca^{2+} concentrations is shown in Figure 3. It is clear that with increasing Ca^{2+} concentration m decreases. This tendency is more pronounced at higher supersaturation ($S > 25$). Therefore the above described acceleration of precipitation decreases with increasing Ca^{2+} concentration. This is in agreement with the fact that an increasing hydrogen carbonate/calcium ratio results in a higher precipitation rate at similar values of supersaturation (Table 1).

These results can be explained by using surface complexation reactions as outlined in the following paragraphs. Calculations of the calcite surface characteristics under experimental conditions was based on the surface

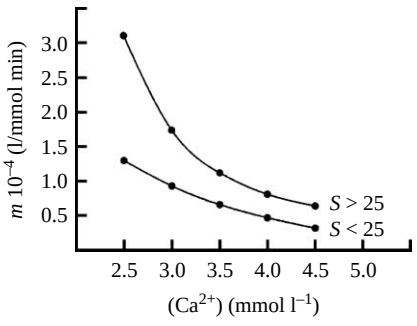

Figure 3 | Calculated slopes $m = dk/dS_{[Ca^{2+}]}$ for the five Ca^{2+} concentrations of the solutions.

Table 2 | Surface complexation reaction and the intrinsic stability constants log K^0_{int} at the calcite/solution interface. > symbolizes the mineral surface (Pokrovsky *et al.* 2000)

Surface complexation reaction	log K^0_{int}
$>CaOH + H^+ = >CaOH_2^+$	11.5
$>CaOH = >CaO^- + H^+$	−12.0
$>CaOH + CO_3^{2-} + 2H^+ = >CaHCO_3^0 + H_2O$	23.5
$>CaOH + CO_3^{2-} + H^+ = >CaCO_3^- + H_2O$	17.1
$>CO_3H = >CO_3^- + H^+$	−5.1
$>CO_3H + Ca^{2+} = >CO_3Ca^+ + H^+$	−1.7

complexation model originally proposed by van Cappellen *et al.* (1993) and later modified by Pokrovsky *et al.* (2000). The surface complexation reactions and their intrinsic stability constants K^0_{int} are summarized in Table 2. In aqueous solutions water molecules are ordered near the calcite surface by forming OH-groups (Perry *et al.* 2007). The precipitation of calcite requires the adsorption of the mineral lattice ions Ca^{2+} and CO_3^{2-} on the surface, followed by dehydration of the formed surface complexes. The major surface species under the experimental conditions described above (pH = 8.30) are $>CaCO_3^-$ and $>CO_3^-$, which were measured by diffuse reflectance infrared spectroscopy (Pokrovsky *et al.* 2000). These results are consistent with the observation that in an aqueous medium the surface charge of calcite is negative (Thomson & Pownall 1989) and that variation in pH does not affect the surface potential significantly (Cicerone *et al.* 1992). Furthermore the surface concentration of $>CaCO_3^-$ and $>CO_3^-$ are positively correlated with observed calcite precipitation rates (Lin & Singer 2005). These results suggest that $>CaCO_3^-$ and $>CO_3^-$ are the dominant species responsible for calcite precipitation. van der Weijden *et al.* (1997) observed a higher growth rate of calcite with increasing HCO_3^-/CO_3^{2-} ratio or decreasing pH, which was explained by a contribution of hydrogen carbonate to calcite crystal growth. This is in line with the fact that dehydration of the mineral surface and the formation of $>CaCO_3^-$ (Table 2) are important steps in calcite precipitation. Therefore it can be concluded that the concentrations of the $>CaCO_3^-$ and $>CO_3^-$ increased with increasing hydrogen carbonate/calcium ratio.

Both Ca^{2+} (aq) ions and $CaCO_3^0$(aq) ion pairs can adsorb to the $>CaCO_3^-$ and $>CO_3^-$ surface species, by the

following reactions:

$$> CaCO_3^- + Ca^{2+}(aq) \rightarrow > CaCO_3 - Ca^+ \quad (13)$$

$$> CaCO_3^- + CaCO_3^0(aq) \rightarrow CaCO_3(s) + > CaCO_3^- \quad (14)$$

$$> CO_3^- + Ca^{2+}(aq) \rightarrow > CO_3 - Ca^+ \quad (15)$$

$$> CO_3^- + CaCO_3^0(aq) \rightarrow CaCO_3(s) + > CO_3^- \quad (16)$$

in which the $CaCO_3^0(aq)$ is about 20 times more reactive than $Ca^{2+}(aq)$ at the calcite–water interface (Nilsson & Sternbeck 1999). However, the dehydration of the dissolved ionic species is required to incorporate lattice ions into the calcite structure during the precipitation process. It can be suggested that the carbonate ion has a greater water exchange rate than the calcium ion and the dehydration of the cation is the rate-determining step in calcite precipitation (Nielsen 1984). The complexation of the cation with a carbonate ligand enhances the dehydration of the remaining water molecules coordinated with the cation (Magerum *et al.* 1978), and thus promotes the adsorption of $CaCO_3^0(aq)$ ion pairs at the $> CaCO_3^-$ and $> CO_3^-$ surface sites.

In Equation (14), $> CaCO_3^-$ on the reactant side is incorporated into the calcite lattice when $CaCO_3^0(aq)$ is adsorbed and dehydrated. The adsorbed $CaCO_3^0(aq)$ becomes a new $> CaCO_3^-$ surface site. Moreover $> CO_3^-$ on the reactant side is incorporated into the calcite lattice, where the remaining CO_3 from $CaCO_3^0(aq)$ becomes a new $> CO_3^-$ surface site (Equation (16)). At these new surface sites further $CaCO_3^0(aq)$ species are adsorbed. With an increasing hydrogen carbonate/calcium ratio the concentration of the adsorbed $CaCO_3^0(aq)$ ion pairs increased resulting in a higher precipitation rate of calcite, as described above. The results are supported by the observation that both the heterogeneous and homogeneous nucleation are independent of the hydrogen carbonate/calcium ratio at similar values of supersaturation. Therefore it can be concluded that solid calcite particles with $> CaCO_3^-$ and $> CO_3^-$ surface species (e.g. enough stable nuclei or calcite seeds) must be present in the solution, because these calcite particles adsorbed the $CaCO_3^0(aq)$ ion pairs.

The observation of Nehrke *et al.* (2007) that the growth was greatest when the ratio CO_3^{2-}/Ca^{2+} in the solution was equal to unity, can be explained by the high and fixed pH value of 10.2. Under this condition the carbonate concentration was probably similar to the hydrogen carbonate concentration and therefore the surface complexation model cannot be applicable. Therefore the results may be explained with the kink growth rate theory for non-Kossel crystals, assuming that the frequency factors for attachment to kink sites are the same for the cation and anion.

CONCLUSIONS

Calcite precipitation experiments were carried out at different supersaturations and different hydrogen carbonate/calcium ratios in an open system, which included the exchange of CO_2 with the atmosphere. Both the heterogeneous and the homogeneous nucleation rate increased with increasing supersaturation. At similar values of supersaturation the hydrogen carbonate/calcium ratio has no significant influence on the nucleation rate. For given Ca^{2+} concentrations it was observed that the precipitation rate increased linearly with increasing supersaturation. This acceleration of the precipitation increased significantly after a certain saturation was exceeded, which suggests a two-dimensional and polynuclear growth mechanism. The accelerations decreased with increasing Ca^{2+} concentrations. This is in accordance with the observation that, in contrast to nucleation, the growth rate increased with increasing hydrogen carbonate/calcium ratio at similar values of supersaturation. The calcite surface complexation model was used to explain the experimental results. An increasing hydrogen carbonate/calcium ratio results in a higher quantity of the dominant $> CaCO_3^-$ and $> CO_3^-$ surface species, resulting in an enhanced growth rate. Furthermore, the dehydration of Ca^{2+} ions and thereby the formation of $CaCO_3^0$ ion pairs, which are adsorbed at the negatively charged calcite surfaces, is promoted by a higher hydrogen carbonate/calcium ratio.

Thus the deposition rate of calcite in natural water systems increased with increasing hydrogen carbonate content and decreasing calcium content at constant supersaturation. Moreover the precipitation rate of $CaCO_3$ in natural water supply as in pipes and heat exchangers increased with increasing hydrogen carbonate/calcium

ratio at similar values of supersaturation. Therefore the supersaturation is not the sole factor controlling calcite precipitation under conditions where Ca^{2+} and HCO_3^- are present as major components.

REFERENCES

Brown, C. A., Compton, R. G. & Narramore, C. A. 1993 The kinetics of calcite dissolution/precipitation. *J. Colloid Interface Sci.* **160**(2), 372–379.

Cicerone, D. S., Regazzoni, P. G. & Blesa, M. A. 1992 Electrokinetic properties of the calcite/water interface in the presence of magnesium and organic matter. *J. Colloid Interface Sci.* **154**(2), 423–433.

Dove, P. M. & Hochella, M. F. 1993 Calcite precipitation mechanisms and inhibition by orthophosphate. In situ observations by scanning force microscopy. *Geochim. Cosmochim. Acta* **57**(3), 705–714.

Drew Ameroid 1997 *Fundamental of Industrial Water Treatment (Grundlagen Der Industriellen Wasserbehandlung)*. Vulkan Verlag, Essen.

Gomez-Morales, J., Torrent-Burgues, J. & Rodrigues-Clemente, R. 1996 Nucleation of calcium carbonate at different initial pH conditions. *J. Cryst. Growth* **169**(2), 331–337.

Gutjahr, A., Dabringhaus, H. & Lacmann, R. 1996 Studies of the growth and dissolution kinetics of the $CaCO_3$ polymorphs calcite and aragonite. I. Growth and dissolution rates in water. *J. Cryst. Growth* **158**(3), 296–309.

House, W. A. 1981 Kinetics of crystallization of calcite from calcium bicarbonate solutions. *J. Chem. Faraday Trans.* **77**(1), 341–359.

Johannsen, K., Alex, H., Burwieck, T., Dorsch, K. & Wichmann, K. 1997 Effect of iron and manganese on the crystal growth of calcium carbonate. *Acta Hydrochim. Hydrobiol.* **25**(4), 202–207.

Kabasaci, S., Althaus, W. & Weinspach, P. M. 1996 Batch precipitation of calcium carbonate from highly supersaturated solutions. *Trans. Inst. Chem. Eng.* **74**, 765–772.

Kazmierczak, T. F., Tomson, M. B. & Nancollas, G. H. 1982 Crystal growth of calcium carbonate. a controlled composition kinetic study. *J. Phys. Chem.* **86**(1), 103–107.

Landolt & Börnstein 1960 *Numerical Values and Functions (Zahlenwerte und Funktionen)* (Vol. II), part 7. In: Bartels, J., Ten Bruggencate, P., Hausen, H., Hellwege, K. H., Schäfer, K. L. & Schmidt, E. (eds). Springer, Berlin Göttingen Heidelberg.

Lin, Y. P. & Singer, P. C. 2005 Effects of seed material and solution composition on calcite precipitation. *Geochim. Cosmochim. Acta* **69**(18), 4495–4504.

Lioliou, M. G., Paraskeva, C. A., Koutsoukos, P. G. & Payatakes, A. C. 2007 Heteregeneous nucleation and growth of calcium carbonate on calcite and quarz. *J. Colloid Interface Sci.* **308**(2), 421–428.

Magerum, D. W., Caley, G. R., Weatherburn, D. C. & Pagenkopf, G. K. 1978 Kinetics and mechanisms of complex formation and ligand exchange. *J. Coord. Chem.* **2**, 1–220. (ed. A. E. Martell).

Mersmann, A., Bartosch, K., Braun, B., Eble, A. & Heyer, C. 2000 Approaches to the predictive estimation of crystallisation kinetics (Möglichkeiten einer vorhersagenden Abschätzung der Kristallisationskinetik). *Chem. Ing. Tech.* **72**(1–2), 17–30.

Meyer, H. J. 1979 Growth rate of calcite in aqueous solutions (Wachstumsgeschwindigkeit von Calcit aus wässrigen Lösungen). *J. Cryst. Growth* **47**(1), 21–28.

Mullin, J. W. 2001 *Crystallisation*. Butterworth Heinemann, Oxford.

Nehrke, G., Reichart, G. J., Van Cappellen, P., Meile, C. & Bijma, J. 2007 Dependence of calcite growth rate and Sr partitioning on solution stoichiometry: Non-Kossel crystal growth. *Geochim. Cosmochim. Acta* **71**(9), 2240–2249.

Nielsen, A. E. 1984 Electrolyte crystal growth mechanisms. *J. Cryst. Growth* **67**(2), 289–310.

Nielsen, A. E. & Toft, M. B. 1984 Electrolyte crystal growth kinetics. *J. Cryst. Growth* **67**(2), 278–288.

Nilsson, Ö. & Sternbeck, J. 1999 A mechanistic model for calcite crystal growth using surface speciation. *Geochim. Cosmochim. Acta* **63**(2), 217–225.

Onsager, L. & Fuoss, R. M. 1932 Irreversible processes in electrolytes. Diffusion, conductance and viscous flow in arbitrary mixtures of strong electrolytes. *J. Phys. Chem.* **36**(11), 2689–2778.

Perry, T. D., Randall, R. T. & Mitchell, R. 2007 Molecular models of a hydrated calcite mineral surface. *Geochim. Cosmochim. Acta* **71**(24), 5876–5887.

Pokrovsky, O. S., Mielczarski, J. A., Barres, O. & Schott, J. 2000 Surface speciation models of calcite and dolomite/aqueous solution interfaces and their spectroscopic evaluation. *Langmuir* **16**(6), 2677–2688.

Reddy, M. M. & Gaillard, W. D. 1981 Kinetics of calcium carbonate (calcite)-seeded crystallization: Influence of solid/solution ratio on the rate constant. *J. Colloid Interface Sci.* **80**(1), 171–178.

Reddy, M. M. & Nancollas, G. H. 1971 The crystallization of calcium carbonate: I. Iisotopic exchange and kinetics. *J. Colloid Interface Sci.* **36**(4), 166–172.

Shiraki, R. & Brantley, S. L. 1995 Kinetics of near-equilibrium calcite precipitation at 100°C. An evaluation of elementary reaction-based and affinity-based rate laws. *Geochim. Cosmochim. Acta* **59**(8), 1457–1471.

Söhnel, O. & Mullin, J. W. 1978 A method for the determination of precipitation induction periods. *J. Cryst. Growth* **44**(3), 377–382.

Söhnel, O. & Mullin, J. W. 1988 Interpretation of crystallization induction periods. *J. Colloid Interface Sci.* **123**(1), 43–50.

Stumm, W. & Morgan, J. J. 1996 *Aquatic Chemistry*. Wiley, New York.

Tai, C. Y., Chang, M. C., Shieh, R. J. & Chen, T. G. 2008 Magnetic effects on $CaCO_3$ crystallization using a commercial magnetic treatment device. *J. Cryst. Growth* **310**(16), 3690–3697.

Takasaki, S., Parsiegla, K. I. & Katz, J. L. 1994 Calcite growth and the inhibiting effect of iron (III). *J. Cryst. Growth* **143**(3–4), 261–268.

Teng, H. H., Dove, P. M. & De Yoreo, J. J. 2000 Kinetics of calcite growth. Surface processes and relationships to macroscopic laws. *Geochim. Cosmochim Acta* **64**(13), 2255–2266.

Thomson, D. W. & Pownall, P. G. 1989 Surface electrical properties of calcite. *J. Colloid Interface Sci.* **131**(1), 74–82.

van Cappellen, P., Charlet, L., Stumm, W. & Wersin, P. 1993 A surface complexation model of the carbonate mineral-aqueous solution interface. *Geochim. Cosmochim. Acta* **57**(15), 3505–3518.

van der Weijden, R. D., van der Heijden, A. E., Witkamp, G. M. & van Rosmalen, G. M. 1997 The influence of total calcium and total carbonate on the growth rate of calcite. *J. Cryst. Growth* **171**(1–2), 190–196.

Zeppenfeld, K. 2001 Experimental studies of the effect of ferriferous corrosion products on calcium precipitation from water containing calcium (Experimentelle Untersuchungen über den Einfluss eisenhaltiger Korrsionsprodukte auf die Kalkabscheidung aus calciumhaltigen Wässern). *Acta Hydrochim. Hydrobiol.* **29**(2–3), 153–163.

Zeppenfeld, K. 2005 Studies of the effect of the flow velocity on calcium carbonate precipitation from water containing calcium (Untersuchungen über den Einfluss der Strömungsgeschwindigkeit auf die Kalkabscheidung aus calciumhaltigen Wässern). *Vom Wasser* **103**(2), 11–19.

First received 29 July 2009; accepted in revised form 22 March 2010